Washington University School of Medicine
Digital Commons@Becker

Open Access Publications

2011

Characterization of a novel, dominant negative KCNJ2 mutation associated with Andersen-Tawil syndrome

Scott B. Marrus
Washington University School of Medicine in St. Louis

Phillip S. Cucilich
Washington University School of Medicine in St. Louis

Wei Wang
Washington University School of Medicine in St. Louis

Jeanne M. Nerbonne
Washington University School of Medicine in St. Louis

Follow this and additional works at: http://digitalcommons.wustl.edu/open_access_pubs

Characterization of a novel, dominant negative *KCNJ2* mutation associated with Andersen-Tawil syndrome

Scott B. Marrus,[1,2,]* Phillip S. Cuculich,[2] Wei Wang[1] and Jeanne M. Nerbonne[1]

[1]Department of Developmental Biology; [2]Department of Internal Medicine; Cardiovascular Division; Washington University School of Medicine; St. Louis, MO USA

Andersen-Tawil syndrome is characterized by periodic paralysis, ventricular ectopy and dysmorphic features. Approximately 60% of patients exhibit loss-of-function mutations in *KCNJ2*, which encodes the inwardly rectifying K$^+$ channel pore forming subunit Kir2.1. Here, we report the identification of a novel *KCNJ2* mutation (G211T), resulting in the amino acid substitution D71Y, in a patient presenting with signs and symptoms of Andersen-Tawil syndrome. The functional properties of the mutant subunit were characterized using voltage-clamp experiments on transiently transfected HEK-293 cells and neonatal mouse ventricular myocytes. Whole-cell current recordings of transfected HEK-293 cells demonstrated that the mutant protein Kir2.1-D71Y fails to form functional ion channels when expressed alone, but co-assembles with wild-type Kir2.1 subunits and suppresses wild-type subunit function. Further analysis revealed that current suppression requires at least two mutant subunits per channel. The D71Y mutation does not measurably affect the membrane trafficking of either the mutant or the wild-type subunit or alter the kinetic properties of the currents. Additional experiments revealed that expression of the mutant subunit suppresses native I_{K1} in neonatal mouse ventricular myocytes. Simulations predict that the D71Y mutation in human ventricular myocytes will result in a mild prolongation of the action potential and potentially increase cell excitability. These experiments indicate that the Kir2.1-D71Y mutant protein functions as a dominant negative subunit resulting in reduced inwardly rectifying K$^+$ current amplitudes and altered cellular excitability in patients with Andersen-Tawil syndrome.

Introduction

Andersen-Tawil syndrome is an autosomal dominant heritable disorder associated with a triad of symptoms: periodic paralysis, ECG changes and characteristic dysmorphic features.[1] Although the genetic cause remains enigmatic in some patients, approximately 60% have been found to have loss of function mutations in *KCNJ2*, the gene which encodes the inwardly rectifying K$^+$ (Kir) pore forming subunit, Kir2.1. This subunit contributes to the inwardly rectifying K$^+$ current (I_{K1}) found in cardiac and a wide variety of other cells.[2]

Although originally identified based on unusual rectification properties and large inward currents at hyperpolarized membrane potentials, inwardly rectifying channels exhibit a smaller, but physiologically crucial, conductance in the more depolarized range of membrane voltages from -80 to -40 mV. In this range, the current plays a role in modulating resting membrane potentials and in shaping the terminal phase of action potential repolarization.[3] Due to these roles, alterations in I_{K1} amplitudes, densities, and/or properties may

stabilize re-entrant malignant arrhythmias such as ventricular fibrillation.[3]

The channels underlying I_{K1} are tetramers of Kir2.x subunits.[1] Kir2.1 (encoded by the KCNJ2 gene) appears to be an essential subunit in ventricular myocytes and Kir2.2 also contributes to I_{K1}.[4] The role(s) of Kir2.3 and 2.4 in cardiac tissue remains less well defined although they have been shown to form heterotetramers with Kir2.1 and/or Kir2.2.[5,6] Channel function is strongly dependent on the membrane-associated second messenger phosphotidylinositolbisphosphate (PIP$_2$), and outward currents are blocked by positively charged intracellular species, most notably polyamines, such as spermine, spermidine and putrescine, and by magnesium ions, thereby generating the property of inward rectification.[1] One intriguing region of the Kir α subunit is the "slide helix" which is predicted to form an alpha helix lying parallel to the cell membrane between the transmembrane and cytoplasmic domains.[7,8] Several Andersen-Tawil syndrome associated mutations have been identified in this region and suggested to disrupt the association of the slide helix region with the regulatory cytoplasmic domain(s).[9]
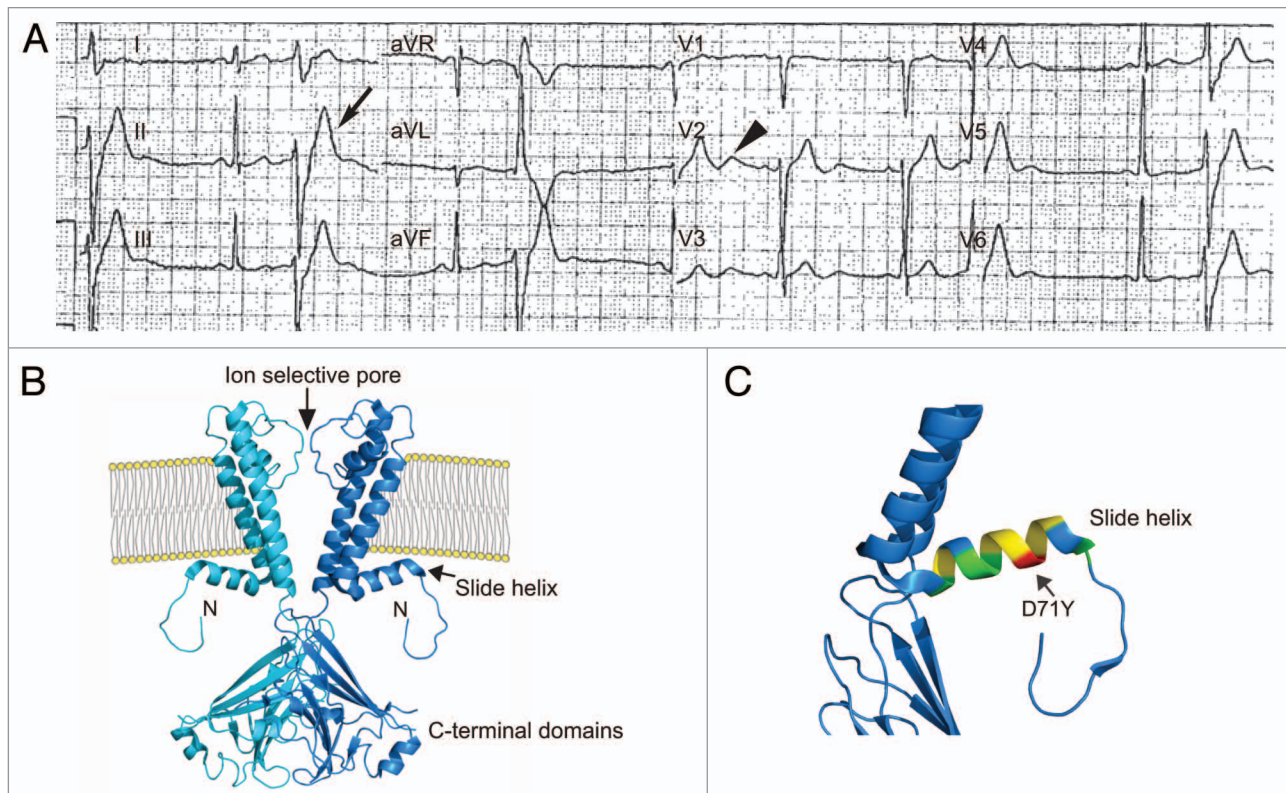
Figure 1. (A) Twelve-lead ECG from the patient demonstrates frequent ventricular ectopy (arrow) and prominent U waves (arrowhead). (B) Predicted structure of Kir2.1 with two subunits of the tetramer removed for clarity. The ion selective pore, slide helix and N- and C-termini are indicated. (C) The slide helix region is shown in greater detail. Colored residues of the slide helix indicate amino acids with hydrophobic side chains (yellow), hydrophilic side chains (green), and the location of the D71Y mutation (red). Structure is based on the KirBac1.1 channel (PBD ID: 1P7B) and rendered using the PyMOL Molecular Graphics System.[25]

Mutations in Kir2.1 have been associated with multiple cardiac electrical diseases, including catecholaminergic polymorphic ventricular tachycardia (CPVT), familial atrial fibrillation, short QT syndrome and Andersen-Tawil syndrome (also called long QT syndrome 7).[1] To date, 33 loss of function mutations in KCNJ2 have been associated with Andersen-Tawil syndrome.[1] Loss of function mutations are located throughout the protein and have been identified in the pore-forming domain, the PIP_2 binding domain, the slide helix and regions involved in protein trafficking.[10]

We report here the identification of a novel *KCNJ2* mutation in a patient with Andersen-Tawil syndrome. In this patient, a single base pair mutation (G211T) results in a D71Y substitution in the slide helix region of Kir2.1. Heterologous expression experiments demonstrate that the mutant subunit fails to form functional Kir channels when expressed alone, but suppress Kir2.1-encoded currents when co-expressed with wild-type Kir2.1 subunits. Co-expression of the mutant subunit, however, does not appear to impair membrane localization of wild-type Kir2.1 subunits or affect the time- or voltage-dependent properties of the currents. Additional experiments demonstrate that expression of hKir2.1-D71Y in mouse neonatal cardiomyocytes suppresses inwardly rectifying currents (I_{K1}), consistent with a functional impact of this mutation on native cardiac I_{K1}. Simulations using a human

ventricular myocyte model predict that the reduction in I_{K1} resulting from the presence of the D71Y mutation will result in prolongation of the terminal portion of the action potential and altered cellular excitability.

Results

Patient presentation. In 2009, a 28-year-old Caucasian male was admitted for further evaluation of periodic paralysis. His symptoms started in January 2005 and resulted in four hospitalizations due to severe muscular weakness. Pertinent findings on examination included bilateral syndactyly of toes 2–3 and ECG tracings revealed frequent premature ventricular complexes and bigeminy (**Fig. 1A**). Although the QTc interval was within normal limits, there were prominent U-waves on the ECG. In light of these combined findings, Andersen-Tawil syndrome was suspected. The *KCNJ2* gene (encoding Kir2.1) was sequenced, revealing a heterozygous, single guanine to thymine base pair change at position 211 (G211T) resulting in a single aspartic acid to tyrosine substitution at position 71 (D71Y). **Figure 1B** shows the overall structure of the Kir2.1 subunit and **Figure 1C** illustrates the slide helix region in more detail.

Kir2.1-D71Y mutation results in a non-functional channel. To assess the functional consequences of the
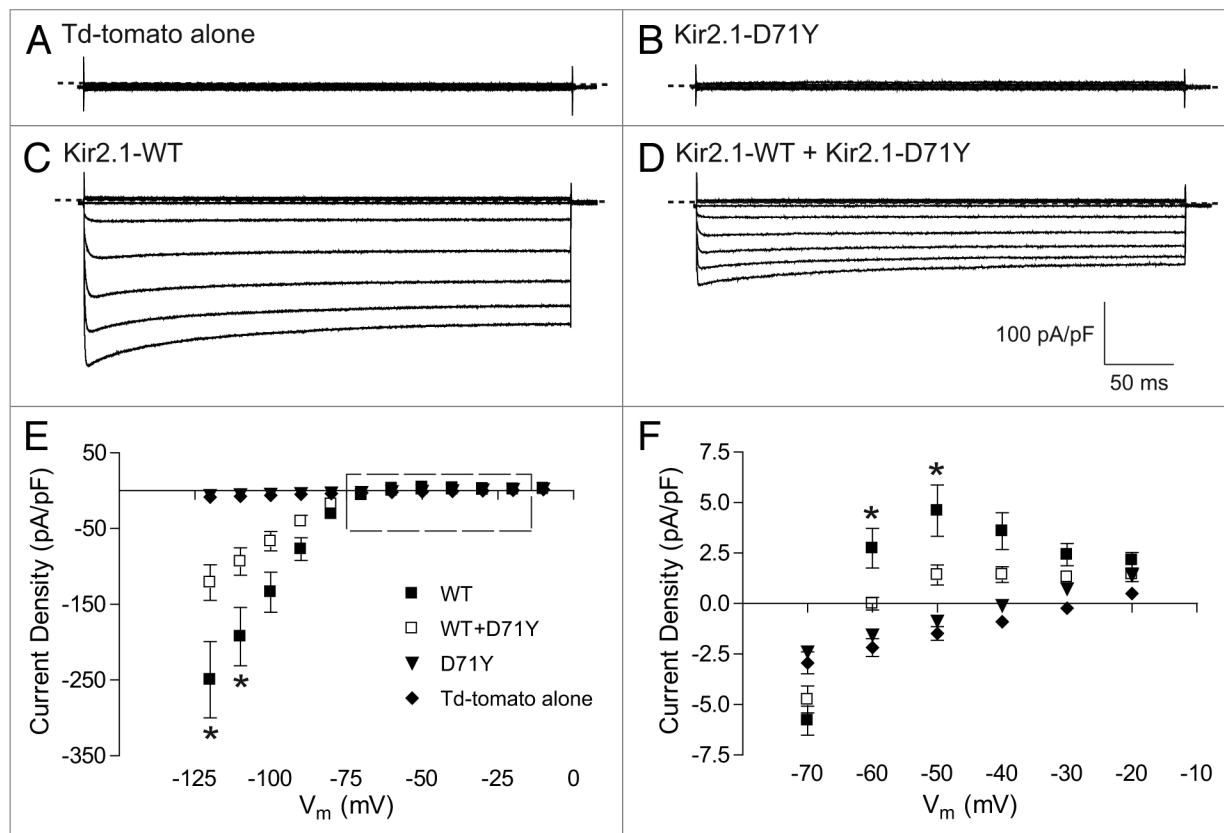
Figure 2. Kir2.1-D71Y fails to form functional channels and suppresses wild-type currents in HEK-293 cells. (A–D) Representative whole cell Kir currents recorded in HEK-293 cells expressing td-tomato alone (A), or in the presence of Kir2.1-D71Y (B), wild-type Kir2.1 (C), or both wild-type Kir2.1 and Kir2.1-D71Y in a 1:1 ratio (D) in response to voltage steps from -120 to -10 mV in 10 mV increments from a holding potential of -70 mV are illustrated. The currents were normalized to cell capacitance (in the same cell) and current densities are plotted; the dotted line indicates 0 pA/pF. (E and F) Current-voltage relationships for the currents measured in HEK-293 cells expressing td-tomato (diamond), Kir2.1-D71Y (triangle), wild-type Kir2.1 (closed squares), or wild-type Kir2.1 and Kir2.1-D71Y in a 1:1 ratio (open squares) are plotted. The voltage range marked by the dashed rectangle in (E) is expanded in (F). All values are means ± SEM. Current densities in cells co-expressing wild-type Kir2.1 and Kir2.1-D71Y were significantly (*p < 0.05) lower than in cells expressing wild-type Kir2.1 alone.

identified Kir2.1-D71Y mutation, HEK-293 cells were transiently transfected with td-tomato together with either wild-type or mutant *KCNJ2* cDNA. Expression of wild-type Kir2.1 resulted in strongly inwardly rectifying currents in HEK-293 cells (**Fig. 2C**) as well as a significant (p < 0.001) hyperpolarization of the resting membrane potential (mean ± SEM = -53 ± 2 mV; n = 21) compared to HEK-293 cells expressing td-tomato alone (-29 ± 2 mV; n = 9). In contrast, expression of Kir2.1-D71Y resulted in only small amplitude currents that were indistinguishable from currents present in HEK-293 cells expressing td-tomato alone (**Fig. 2A**); mean ± SEM peak current densities at -120 mV in cells expressing td-tomato alone (-8.4 ± 1.4 pA/pF) or td-tomato plus Kir2.1-D71Y (-6.4 ± 0.5 pA/pF) were not significantly different. Expression of either wild-type Kir2.1, mutant Kir2.1, or co-expression of wild-type and mutant Kir2.1 did not result in significant changes in cell membrane capacitance or membrane resistance (data not shown).

Co-expression of Kir2.1-D71Y with wild-type Kir2.1 results in a reduction of the wild-type current. Because the phenotypic manifestations of Andersen-Tawil syndrome are evident in heterozygous carriers of *KCNJ2* mutations, we next investigated the consequences of co-expression of Kir2.1-D71Y with wild-type Kir2.1 (**Fig. 2**). Co-expression of the wild-type and mutant subunits in a 1:1 ratio resulted in significantly smaller currents (**Fig. 2D**) compared to expression of the same amount of the wild-type subunit alone (**Fig. 2C**). For example, the mean ± SEM inward current density at -120 mV was reduced significantly (p = 0.02) from -249.5 ± 50.3 pA/pF (n = 21) in cells expressing wild-type Kir2.1 to -121.3 ± 23.5 pA/pF (n = 22) in cells co-expressing wild-type Kir2.1 and Kir2.1-D71Y (**Fig. 2E**). Similarly, the mean ± SEM outward current density at -50 mV was reduced (p = 0.01) from 4.6 ± 1.3 pA/pF in cells expressing wild-type Kir2.1 to 1.4 ± 0.5 pA/pF in cells co-expressing wild-type Kir2.1 and Kir2.1-D71Y (**Fig. 2F**). Co-expression of Kir2.1-D71Y with wild-type Kir2.1 also resulted in a small depolarizing shift in the resting membrane potential (-46.8 ± 3.0 mV) compared with cells expressing only wild-type Kir2.1 (-53.4 ± 1.3 mV), although this trend was not statistically significant (p = 0.09). Taken together, these observations suggest that Kir2.1-D71Y functions as a dominant negative subunit capable of suppressing the function of wild-type Kir2.1 subunits.
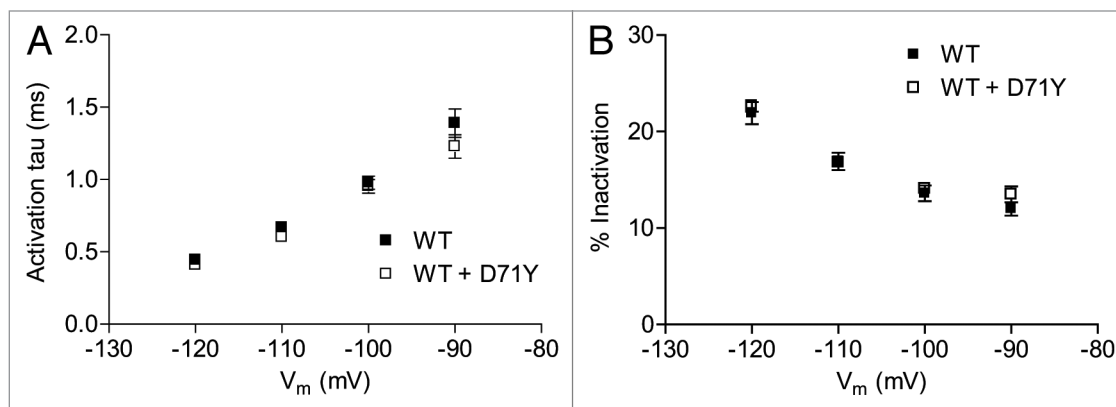
Figure 3. Voltage-dependent activation and inactivation of currents produced by co-expression of wild-type Kir2.1 and Kir2.1-D71Y are indistinguishable from currents produced by expression of wild-type Kir2.1 alone. (A) The time course of inward current activation was fitted with a single exponential and the mean ± SEM time constants (tau) are plotted as a function of membrane voltage. (B) Mean ± SEM percent inactivation determined at each voltage are plotted as a function of test potential.

Kir2.1-D71Y does not alter current kinetics. One possible mechanism by which mutant subunit co-assembly with wild-type subunits could result in decreased currents might be by increasing the binding affinity for one or more of the cytoplasmic agents (polyamines and magnesium) responsible for blocking outward currents through Kir2.1 channels.[1] To explore this possibility, the activation phases of the inward currents at hyperpolarized potentials, which reflect the unbinding of magnesium and polyamines from the pore,[11] were examined. Analyses of the time course of inward current activation revealed an essentially instantaneous phase followed by a slower phase that was well-described by a single exponential; there were no improvement in the fits when multiple exponential terms were included. The amplitude of the instantaneous phase represented approximately 70% of the peak current for both wild-type (72 ± 1%, n = 20) and wild-type:D71Y heteromeric channels (74 ± 2%); these values are not significantly different. The time course of the slower phase of activation is voltage dependent as previously described in reference 11, and the activation time constants were indistinguishable for wild-type and wild-type:D71Y currents (**Fig. 3A**). The mean ± SEM activation tau at -120 mV, for example, was 0.44 ± 0.03 ms in cells expressing wild-type Kir2.1 and 0.40 ± 0.02 ms in cells co-expressing wild-type and D71Y Kir2.1 (**Fig. 3A**).

Kir2.1 mediated currents also exhibit partial inactivation, as evidenced by the attenuation of current from the initial peak to a steady state plateau during a voltage step and, as previously described in reference 12, the extent of the inactivation is voltage dependent (**Fig. 2C**). Fractional current inactivation was quantified here by calculating the ratio of the peak current to the steady state current. There were no significant differences between the fractional inactivation of wild-type Kir2.1 and wild-type Kir2.1 + Kir2.1-D71Y currents at any test potential (**Fig. 3B**). At -120 mV, for example, the percent current inactivation during the 350 ms voltage step was 22 ± 1% for wild-type Kir2.1 (n = 20) and 23 ± 1% for wild-type Kir2.1 + Kir2.1-D71Y (n = 22). Together, these observations demonstrate that I_{K1} in the presence of Kir2.1-D71Y exhibits normal current kinetics; reflecting either that the mutant subunits do not alter channel kinetics or that channels containing one or more mutant subunits are non-functional and the functional channels are entirely wild type (see Discussion).

Dominant-negative suppression of currents requires co-assembly of mutant and wild-type subunits. It has previously been shown that Kir2.1 subunits assemble as tetramers.[1] Subsequent experiments here, therefore, were aimed at determining the minimal number of mutant subunits necessary to suppress channel function by co-transfecting HEK-293 cells with wild-type and mutant subunits in varying proportions. Theoretical curves were constructed to predict the expected current for each wild-type:mutant subunit ratio based on the assumptions that: (1) the proportions of wild-type and mutant subunit proteins in each cell reflects the relative proportion of the transfected wild-type and mutant cDNA constructs and (2) the probability of incorporation of a mutant subunit into a channel is equivalent to the proportion of mutant subunits expressed in the cell. A separate theoretical curve was generated for the scenarios in which 1, 2, 3 or 4 mutant subunits are required to reduce channel function. As shown in **Figure 4**, the experimental data deviate significantly from the curve predicted for only one mutant subunit being required to eliminate channel function, suggesting that more than one mutant subunit per channel complex is required to reduce channel function.

Membrane trafficking of Kir2.1-D71Y containing channels. One possible mechanism to account for the observed decrease in K+ currents when the Kir2.1-D71Y mutant subunit is co-expressed with the wild-type subunit (**Fig. 2**) is that there is reduced membrane trafficking of wild-type:mutant Kir2.1 multimers compared with wild-type Kir2.1 homomeric channels.[10] To examine the membrane trafficking of Kir2.1-containing channels directly, tagged subunits were constructed as described in Methods. Briefly, an in-frame C-terminal YFP tag was added to the Kir2.1-D71Y subunit and an in-frame C-terminal myc tag was added to the wild-type Kir2.1 subunit; both constructs were expressed in HEK-293 cells. Similar to the untagged wild-type Kir2.1 subunits, expression of Kir2.1-myc subunits resulted in robust inwardly rectifying currents (**Fig. 5A**) whereas expression of tagged Kir2.1-D71Y-YFP failed to result in any measureable

currents (**Fig. 5C**). Co-expression of Kir2.1-myc subunits with untagged Kir2.1-D71Y subunits resulted in a suppression of the current as was seen with untagged subunits (**Fig. 5B**). The mean ± SEM peak current density at -120 mV was -598.2 ± 111.7 pA/pF (n = 11) in cells expressing Kir2.1-myc and -239.6 ± 45.5 pA/pF in cells co-expressing Kir2.1-myc and Kir2.1-D71Y (p = 0.02). Staining of cells expressing the wild-type Kir2.1-myc subunit revealed anti-myc staining at the cell surface (**Fig. 5D**). In addition, the anti-myc staining was also present in cells co-expressing wild-type Kir2.1-myc and Kir2.1-D71Y (**Fig. 5E**), demonstrating that membrane localization of wild-type Kir2.1 subunits persists despite the marked reduction of currents in cells co-expressing the dominant negative Kir2.1-D71Y subunit. Interestingly, in cells expressing YFP-tagged Kir2.1-D71Y subunit, YFP fluorescence was evident at the cell surface despite the lack of detectable currents (**Fig. 5F**). These results clearly suggest that the decrease in Kir2.1-mediated currents does not result from mislocalization of the Kir (wild-type or D71Y mutant) subunits.

Suppression of native I_{K1} in mouse neonatal cardiomyocytes. Ion channel function reflects the interactions of multiple pore-forming and accessory subunits as well as signaling cascades, many of which remain incompletely characterized.[13] However, these modulatory components are often lacking in non-excitable heterologous cell systems such as HEK-293 cells. To explore the physiological relevance of our observations in HEK-293 cells, we utilized mouse neonatal cardiomyocytes that express a native I_{K1} composed of Kir2.1 and Kir2.2.[4] Transfection of isolated neonatal cardiomyocytes with td-tomato and the human *KCNJ2-G211T* cDNA construct resulted in a marked decrease in I_{K1} density compared to cells transfected with td-tomato alone (**Fig. 6**). The mean ± SEM peak inward current density at -120 mV was -3.3 ± 0.5 pA/pF (n = 15) in cells expressing Kir2.1-D71Y compared to -8.7 ± 3.3 pA/pF (n = 23) in cells expressing td-tomato alone (p < 0.0001). The Kir2.1-D71Y mutation, therefore, functions as a dominant negative mutation in an intact cellular context. Interestingly, despite the decrease in I_{K1}, the resting membrane potential remained unchanged (-41 ± 2 mV in cells expressing Kir2.1-D71Y compared to -43 ± 2 mV in cells expressing td-tomato, p = NS).

Simulations predict the effects of I_{K1} reduction in human ventricular myocytes. To determine the functional consequences of I_{K1} reduction in human cardiac myocytes, we utilized a recently published model which accurately reproduces the normal repertoire of ionic currents and behavior of the human ventricular myocyte.[14] As discussed above, the residual current in the presence of Kir2.1-D71Y exhibits normal kinetic features; therefore, I_{K1} kinetics in the model were not changed and the peak current amplitude was scaled to reproduce the effects of the Kir2.1 mutations. Reduction of I_{K1} amplitude resulted in action potential prolongation; notably, this prolongation was confined to the terminal portion of the action potential (**Fig. 7A and Table 1**). For example, 50% reduction of I_{K1} resulted in no significant changes in APD30 or APD50 whereas APD90 was prolonged by 5% and APD99 by 13% (**Table 1**). In addition, no change in resting membrane potential or action potential amplitude occurred with reduction of I_{K1} amplitude (**Table 1**).
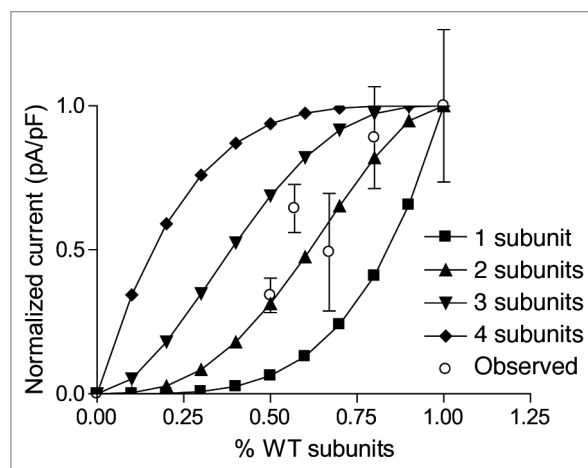

Figure 4. Wild-type and D71Y Kir2.1 subunits co-assemble in a complex requiring at least 2 mutant subunits to reduce wild-type channel function. Theoretical curves (solid symbols) were constructed predicting the current resulting from a given percentage of wild-type subunits under the assumption that 1, 2, 3 or 4 D71Y subunits are required to reduce channel function. Recorded currents, resulting from varying the percentage of wild-type subunits (50% WT, n = 11; 60% WT, n = 7; 70% WT, n = 7; 80% WT, n = 9; WT, n = 8), are superimposed in open circles. All data are means ± SEM. (See text and methods for further details).

One possibility is that changes in I_{K1} might affect the action potential threshold and thus contribute to the increase in ventricular ectopy, which occurs in Andersen-Tawil patients. **Figure 7B** shows the amplitude-duration curve for stimuli which result in triggered action potentials; only a trivial reduction in rheobase (39 vs. 40 pA/pF) resulted from a 90% decrease in I_{K1} amplitude. However, subthreshold stimulations resulted in a significantly longer depolarization before the membrane voltage returned to the resting level when I_{K1} levels were reduced. **Figure 7C** shows illustrative examples in which a 90% reduction in I_{K1} results in prolonged depolarizations in response to subthreshold stimuli. Similar changes of a smaller magnitude were observed after a 50% reduction in I_{K1} amplitude (data not shown). In the context of an intact heart, these depolarizations could increase the likelihood that a simultaneous, sub-threshold second stimulus would generate an action potential and thus offer an explanation of the prevalence of ectopic beats observed in patients with Andersen-Tawil syndrome.

Discussion

With the proliferation of disease associated mutations, it is becoming increasingly important to determine whether an identified genetic variant is pathologic or represents background genetic noise.[15] The results reported here support the conclusion that the novel *KCNJ2-G211T* genetic variant identified in a patient with Andersen-Tawil syndrome is a loss of function mutation responsible for the patient's disease. Experiments conducted in heterologous cells revealed that the Kir2.1-D71Y mutant subunit co-assembles with wild-type Kir2.1 subunits and suppresses currents without detectable effects on membrane
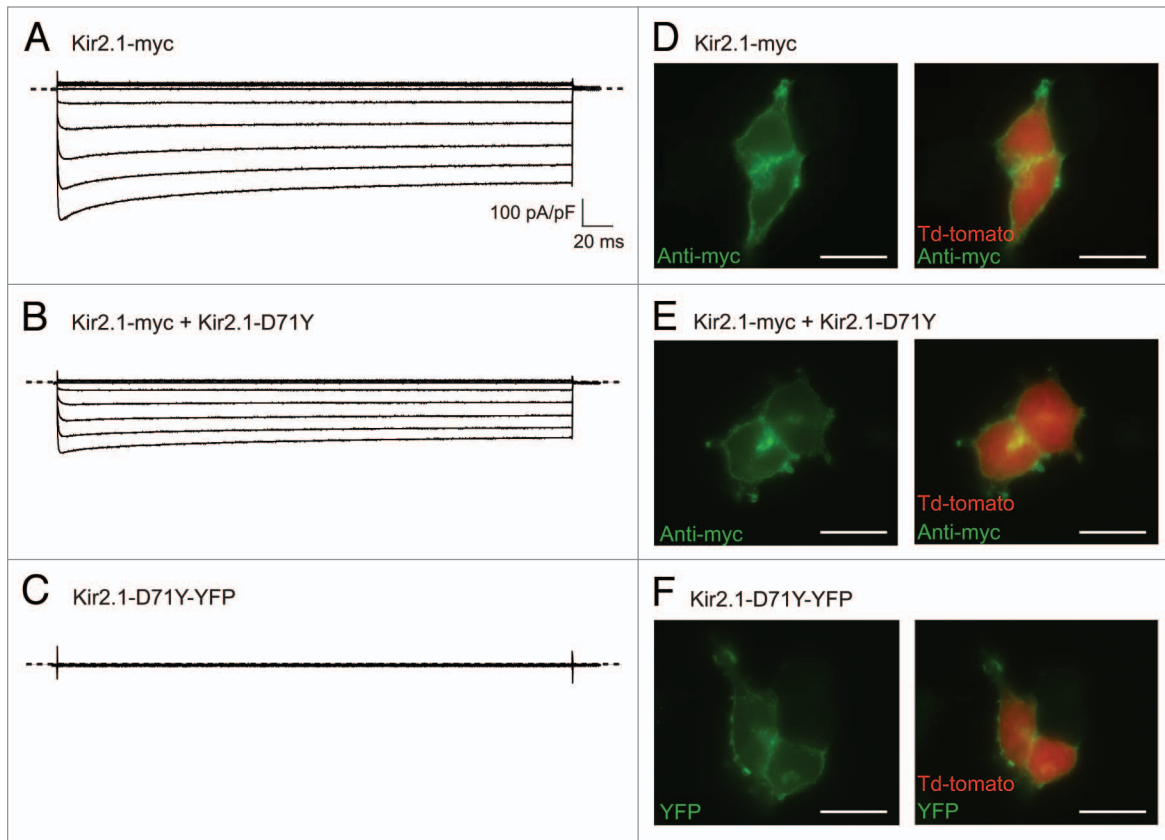
Figure 5. Both mutant and wild-type Kir2.1 subunits localize to the cell surface in HEK-293 cells. Representative whole cell currents recorded from HEK-293 cells expressing td-tomato with Kir2.1-myc (A), Kir2.1-myc + Kir2.1-D71Y (B) or Kir2.1-D71Y-YFP (C) in response to voltage steps from -120 mV to -10 mV (10 mV increments) from a holding potential of -70 mV were normalized to cell capacitance and plotted; the dotted line indicates 0 pA/pF. (D) In cells expressing wild-type Kir2.1-myc alone, anti-myc staining is evident at the cell surface. (E) Anti-myc staining is also evident at the cell surface when wild-type Kir2.1-myc was co-expressed with the mutant Kir2.1-D71Y. (F) When expressed alone, the mutant Kir2.1-D71Y-YFP subunit is also evident at the cell surface. For all parts, the (wild-type or mutant) Kir2.1 subunit staining contrasts with the cytoplasmic td-tomato fluorescence. Scale bar = 60 μm.
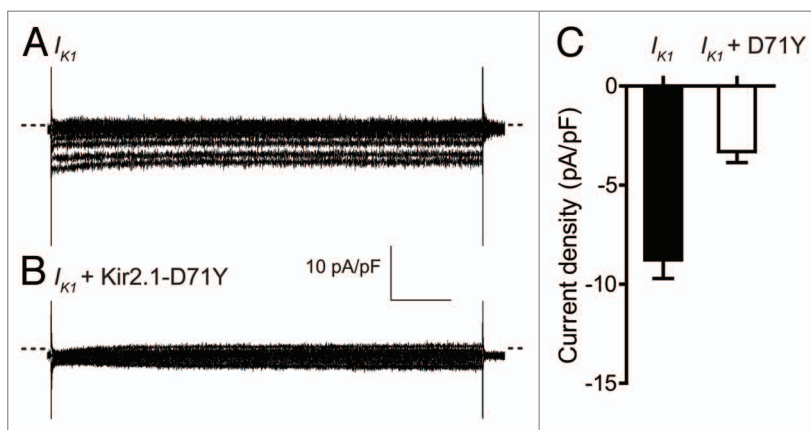

Figure 6. Native I_{K1} in neonatal mouse ventricular myocytes is suppressed by expression of Kir2.1-D71Y. (A and B) Representative Kir currents recorded from mouse neonatal myocytes transfected with td-tomato alone (A) and in the presence of human Kir2.1-D71Y (B) in response to voltage steps from -120 mV to -40 mV in 10 mV increments from a holding potential of -70 mV and normalized to cell capacitance. (C) Mean ± SEM peak native I_{K1} density measured at -120 mV in cells transfected with td-tomato alone (solid bar) and in the presence of human Kir2.1-D71Y (open bar).

trafficking of channel subunits or current kinetics. Additional experiments demonstrated that the human Kir2.1-D71Y subunit suppresses native I_{K1} in mouse neonatal cardiomyocytes, providing further support that this mutation results in I_{K1} channel dysfunction in vivo. Simulations predict that in the context of the human ventricular myocyte, this mutation will result in action potential prolongation and no change in the resting membrane potential but a decreased stability of the membrane voltage resulting in prolonged sub-threshold depolarizations.

Physiological roles of Kir2.1. There is general consensus that Kir2.1 plays important roles in regulating the electrical excitability of both cardiac and skeletal muscle, although several previous studies have provided conflicting results regarding the role of Kir2.1 mediated currents in the generation of cardiomyocyte resting membrane potentials.[4,16] The results of the experiments completed here, however, demonstrated that neither the co-expression
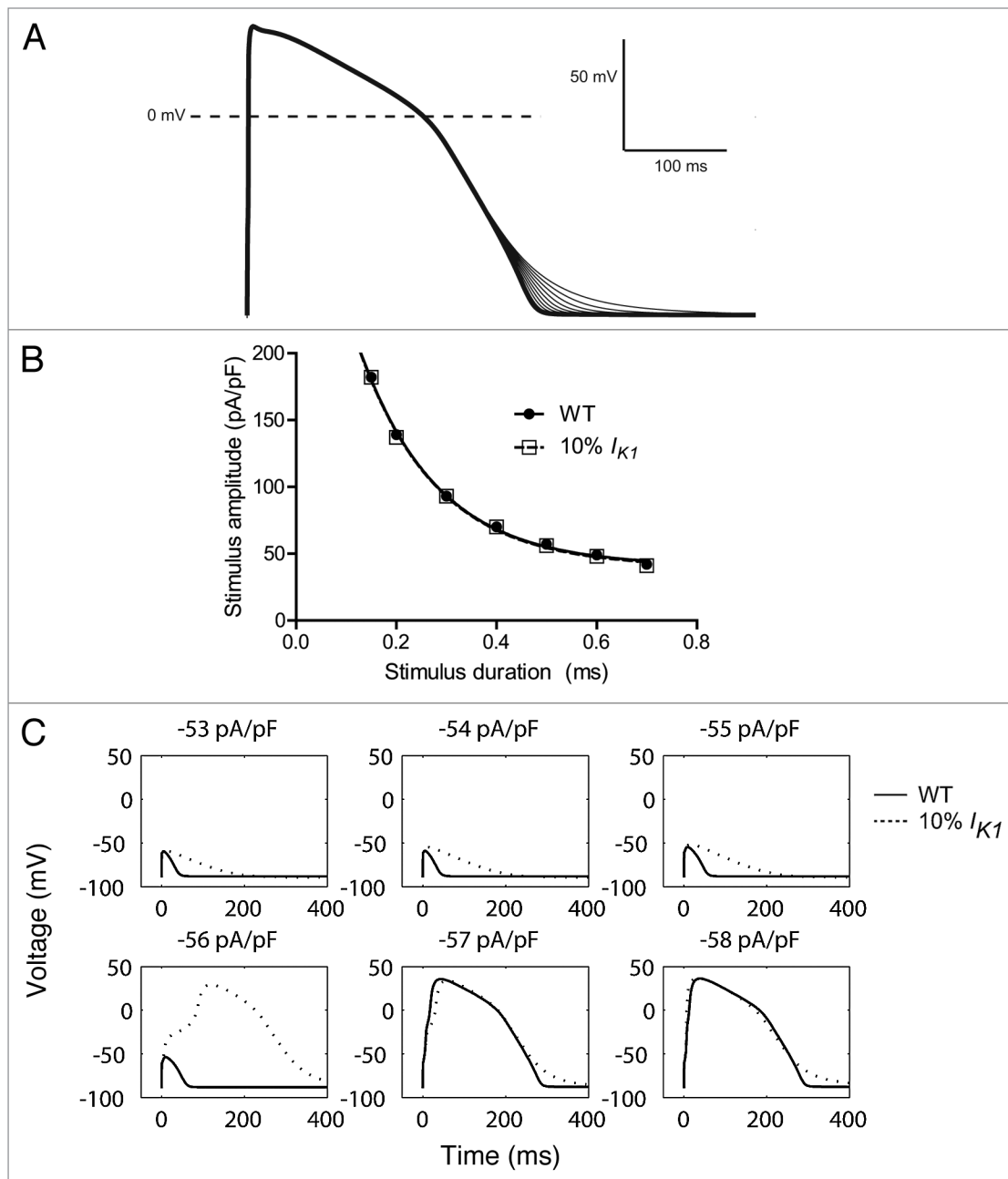
Figure 7. Human ventricular myocyte simulations. (A) The simulated steady-state action potential in wild-type cells (heavy line) is shown with a family of superimposed action potentials (light lines) predicted to result from progressive decreases in I_{K1} amplitude in 10% increments. (B) Amplitude-duration relationship for triggered action potentials is shown for wild-type (solid symbols and line) and cells with a 90% decrease in I_{K1} amplitude (open symbols and dotted line). (C) Membrane potential response to stimuli of varying amplitude (as indicated in each part) in both wild-type cells (solid line) and cells with 90% reduction in I_{K1} (dotted line) demonstrating both a small change in action potential threshold and prolonged membrane depolarization in response to sub-threshold stimuli as a result of I_{K1} reduction.

of wild-type and mutant Kir2.1 subunits in HEK-293 cells nor the expression of the mutant Kir2.1-D71Y in mouse neonatal cardiomyocytes resulted in a significant change in resting membrane potential despite suppressing Kir2.1 mediated currents. In conjunction with modeling data failing to predict a change in human cardiomyocyte resting membrane potential, these results suggest that the *KCNJ2-G211T* mutation likely does not exert its pathologic effects via a change in resting membrane potential.

Despite the lack of effect on resting membrane potential, I_{K1} could play a role in membrane stability and excitability. Due to the fact that cellular excitability depends on the aggregate effects of an array of species-specific ion channels, an in silico model of the human ventricular myocyte was used to explore the role of I_{K1} in membrane stability. Interestingly, simulation results indicated that I_{K1} plays an important role in the rate at which the membrane returns to the resting potential after a perturbation.

Table 1. Simulated action potential parameters resulting from I_{K1} reduction in a human ventricular myocyte model

	Wild-type	50% I_{K1} reduction	90% I_{K1} reduction
Resting V_m (mV)	-88	-88	-89
Action potential amplitude (mV)	128	128	130
APD30 (ms)	165	164	164
APD50 (ms)	207	206	207
APD90 (ms)	266	278	304
APD99 (ms)	286	322	552

No significant change occurred in resting membrant potential (V_m), action potential amplitude, or action potential duration measured at 30% or 50% repolarization (APD30 and APD50) whereas action potential duration at 90% and 99% repolarization (APD90 and APD99) was prolonged.

Sub-threshold stimuli resulted in a prolonged depolarization in the setting of I_{K1} reduction. This finding suggests a novel mechanism by which I_{K1} reduction contributes to arrhythmias, i.e., by generating sub-threshold depolarizations that could summate to result in ectopic activation.

Inwardly rectifying K$^+$ currents have also been suggested to play an important role in the repolarization phase of the action potential and in the stability of ventricular arrhythmias.[3] Previous studies using either knock-out or dominant-negative strategies in mice and guinea pig have demonstrated action potential prolongation.[4,16,17] In this study, the human cardiac myocyte model predicted action potential prolongation confined to the terminal portion of the action potential. This finding is consistent with published results on guinea pig cardiomyocytes but contrasts with studies of mouse cardiomyocytes which exhibited action potential prolongation at both APD50 and APD90.[4,17] These observations emphasize the potentially species-specific nature of electrophysiological perturbations reflecting differences in ion channel expression and function.

Kir2.1, as well as many related Kir family members, is expressed in a wide variety of tissues, a fact that is consistent with the clinical observations that patients harboring mutations in *KCNJ2* exhibit a complex phenotype affecting multiple tissues.[2] The patient carrying this *KCNJ-G211T2* mutation suffered periodic paralysis, cardiac ectopy and skeletal abnormalities consistent with a role for Kir2.1 channels in the function of skeletal muscle, cardiac myocytes and bone development. It has been shown that inward rectifying currents are present in osteoclasts where they are believed to offset the hyperpolarization induced by proton export.[2] In addition to its role in electrical excitability, Kir2.1 expression in skeletal muscle is involved in myotube fusion.[2]

Kir2.1 structure and function. Andersen-Tawil syndrome associated mutations have been reported throughout the sequence of KCNJ2, including the transmembrane helices, the ion selectivity filter, the slide-helix and the N- and C-termini.[18] Most of the identified Andersen-Tawil syndrome associated mutations result in dominant-negative suppression of wild-type Kir2.1-mediated currents through multiple mechanisms. Previous KCNJ2 mutations located in the PIP$_2$ binding domain have been shown to

alter PIP$_2$ affinity,[19] a mutation in the slide helix has been shown to alter both magnesium and PIP$_2$ sensitivity,[20] and mutations in multiple regions have been associated with altered membrane localization.[10,21] Interestingly, additional mutations located in the slide helix region have been shown to function as dominant negative loss of function mutations without affecting membrane localization or PIP$_2$ binding affinity.[9] Similar to several previously reported mutations,[9] the D71Y mutation reported here is located in the slide helix region of the Kir2.1 (**Fig. 1B**) and does not affect membrane localization. In addition, we report here that the presence of D71Y mutation has no effect on current kinetics, indicating that either this region does not directly participate in channel gating or that this mutation renders the channel entirely non-functional, thus leaving a (normal) residual current composed of solely wild-type subunits.

Methods

cDNA constructs. A cDNA encoding human *KCNJ2* was obtained from Open Biosystems and a PCR product containing the open reading frame with added EcoR1 and Xho1 sites was subcloned into the mammalian expression vector pCMV Script (Clontech). PCR site-directed mutagenesis was carried out using the QuickChange XL kit (Stratagene); the mutated gene was subcloned into pCMV Script and the final construct was sequenced to verify the mutation and to exclude PCR errors. In addition, the *KCNJ2* cDNA was subcloned into pCMV c-myc (Clontech) and the *KCNJ2-G211T* cDNA was subcloned into pEYFP-N1 (Clontech) to generate myc- and YFP-tagged subunits, respectively.

Cell culture and transfections. Human embryonic kidney-293 (HEK-293) cells were maintained in Dulbecco's Modified Eagle Medium (DMEM-Gibco, Invitrogen, 11965) supplemented with 5% fetal bovine serum (Atlas Biological, FP-0500-A), 5% horse serum (Gibco, Invitrogen, 26050), and penicillin/streptomycin (Gibco, Invitrogen, 15140) in a 37°C 95% air/5% CO$_2$ incubator. Mouse neonatal cardiomyocytes were isolated from post-natal day 1–3 pups anesthetized with isoflurane and euthanized by decapitation. After removing the hearts, ventricles were dissected and minced in Hanks Balanced Salt Solution (HBSS), containing in mM: 127 NaCl (Sigma, S5886), 5.4 KCl (Sigma, P9541), 4.2 NaHCO$_3$ (Sigma, S5761), 0.4 Na$_2$HPO$_4$ (Sigma, S5011), 0.44 KH$_2$PO$_4$ (Sigma, P5655), 5.5 glucose (Sigma, G6152), and penicillin/streptomycin. The ventricular pieces were incubated overnight in HBSS containing 0.1% trypsin (T8003, Sigma) followed by a 30 min incubation at 37°C. The tissue was triturated, centrifuged at 300x g, and resuspended in DMEM supplemented with 20% fetal calf serum and penicillin/streptomycin. Cells were plated on tissue culture plates for 1 h at 37°C to allow adhesion of fibroblasts. Cells in suspension were then plated on collagen (type 1, Sigma, C9791)-coated coverslips at low density and transfected after 24 h incubation at 37°C.

Transient transfections were carried out using Lipofectamine 2000 (Invitrogen) as previously described in reference 22. All transfections were performed with 1 μg of wild-type vector, variable amounts of mutant vectors, and variable amounts of

empty vector to result in a total of 2 μg of DNA in all transfections. Additionally, 0.25 μg of pCMV-td-tomato plasmid was added to all transfections to allow identification of transfected cells.

Whole-cell recordings. Twenty-four to 36 h (for HEK-293 cells) or 24–48 h (for neonatal myocytes) after transfection, whole-cell K$^+$ currents were recorded at room temperature (20–23°C) using previously described solutions and protocols.[22,23] Recording pipettes fashioned from borosilicate glass (WPI, TW150F-4) had resistances of 2–3 MΩ when filled with recording solution. Experiments were controlled by and data were collected using an Axopatch 1D, digitized with a Digidata 1322A and stored on a Gateway PC running Clampex 9.2 (all Molecular Devices).

Data analysis. Data were analyzed using ClampFit (Molecular Devices), Excel (Microsoft) and Prism (GraphPad). Only cells with a membrane resistance >300 MΩ and an access resistance <15 MΩ were analyzed. Membrane capacitance and input resistance were measured by analyzing the decay phases of the capacitive current elicited by a 20 ms voltage step (±10 mV) from a holding potential of -40 mV, as described previously in reference 23. Peak Kir currents were measured by averaging the current during 10 ms at the maximal current evoked at each test potential. Steady state Kir currents were measured 340 ms after the onset of the voltage steps. Instantaneous Kir currents were measured at the end of the initial capacitive transient. The time course of current activation was determined by fitting the current trace from the end of the capacitive transients to the peak current with a mono-exponential function. All data were tested for normalcy and subsequently analyzed with a one- or two-way ANOVA, Kruskal-Wallis, unpaired t-test or Mann-Whitney U test as appropriate. All results are reported as means ± SEM.

Immunohistochemistry. Thirty-six hours after transfections, HEK-293 cells were washed in phosphate buffered saline (PBS) and fixed with 4% paraformaldehyde for 20 min. Cells were incubated for 1 h in blocking buffer (PBS with 5% goat serum and 0.2% Triton X-100) followed by incubations with primary and secondary antibodies [1:1,000 mouse anti-myc monoclonal antibody (Millipore), 1:1,000 Alexa 488 goat anti-mouse antibody (Invitrogen)] in blocking buffer for 1–2 h each at room temperature. After washing in PBS, coverslips were mounted in ProLong Gold antifade solution (Invitrogen). Cells were imaged on a Nikon Eclipse inverted microscope equipped with a CoolSNAP CCD (Photometrics); images were acquired using Volocity 4 (Improvision, PerkinElmer) software.

Calculation of channel stochiometry. The number of mutant subunits required to reduce channel function was estimated using previously described methods in reference 24. Briefly, the distribution of possible combinations of four subunits, each of which can be either wild-type or mutant, follows a binomial distribution. The probability of a channel containing 1, 2, 3 or 4 mutant subunits can be calculated from the probability mass function

$$P_k = \left(\frac{n!}{k!\,(n-k)!}\right) p^k (1-p)^{n-k}$$

where P_k = probability that a channel contains k mutant subunits, n = total number of subunits, k = number of mutant subunits and p = probability of incorporation of a mutant subunit (assumed to be equal to the proportion of transfected mutant cDNA). Assuming that the decrease in current is proportional to the percentage of dysfunctional channels, this allows the generation of a family of theoretical curves predicting the decrease in current based on the hypotheses that one, two, three or four mutant subunits are required to reduce channel function. The current resulting from different ratios of wild-type and mutant subunits is then recorded and the data fit to the best theoretical curve.

Simulations. Simulations were carried out using a model of human endocardial ventricular myocytes using the published O'Hara-Rudy dynamic model[14] with the addition of a scaling factor to reduce I_{K1} amplitude. All simulations were carried out for 1,000 beats to ensure steady state conditions. Amplitude-duration curves were constructed by determining the minimal stimulus amplitude required to trigger an action potential for each stimulus duration; the resulting curve was fitted with a single exponential function, using Prism to determine the rheobase.

Conclusion

In summary, the experiments presented here demonstrate that a novel *G211T* mutation in *KCNJ2* identified in a patient with all of the cardinal features of Andersen-Tawil syndrome results in the production of mutant Kir2.1-D71Y protein that functions as a dominant negative to suppress endogenous I_{K1}. The mutant subunit reduces wild-type Kir2.1 currents in both HEK-293 cells and neonatal mouse cardiomyocytes, without measureable effects on membrane localization, current kinetics or resting membrane potentials. Simulations predict that these effects would lead to a prolongation of the human cardiomyocyte action potential and to destabilization of the resting membrane potential. These observations are interpreted as suggesting that this mutation is responsible for the patient's clinical syndrome.

References

1. Anumonwo JM, Lopatin AN. Cardiac strong inward rectifier potassium channels. J Mol Cell Cardiol 2009; 48:45-54.

2. Jongsma HJ, Wilders R. Channelopathies: Kir2.1 mutations jeopardize many cell functions. Curr Biol 2001; 11:747-50.

3. Dhamoon AS, Jalife J. The inward rectifier current (I_{K1}) controls cardiac excitability and is involved in arrhythmogenesis. Heart Rhythm 2005; 2:316-24.

4. Zaritsky JJ, Redell JB, Tempel BL, Schwarz TL. The consequences of disrupting cardiac inwardly rectifying K^+ current (I_{K1}) as revealed by the targeted deletion of the murine Kir2.1 and Kir2.2 genes. J Physiol 2001; 533:697-710.

5. Preisig-Muller R, Schlichthorl G, Goerge T, Heinen S, Bruggemann A, Rajan S, et al. Heteromerization of Kir2.x potassium channels contributes to the phenotype of Andersen's syndrome. Proc Natl Acad Sci USA 2002; 99:7774-9.

6. Schram G, Melnyk P, Pourrier M, Wang Z, Nattel S. Kir2.4 and Kir2.1 K^+ channel subunits co-assemble: a potential new contributor to inward rectifier current heterogeneity. J Physiol 2002; 544:337-49.

7. Enkvetchakul D, Jeliazkova I, Bhattacharyya J, Nichols CG. Control of inward rectifier K channel activity by lipid tethering of cytoplasmic domains. J Gen Physiol 2007; 130:329-34.

8. Kuo A, Gulbis JM, Antcliff JF, Rahman T, Lowe ED, Zimmer J, et al. Crystal structure of the potassium channel KirBac1.1 in the closed state. Science 2003; 300:1922-6.

9. Decher N, Renigunta V, Zuzarte M, Soom M, Heinemann SH, Timothy KW, et al. Impaired interaction between the slide helix and the C-terminus of Kir2.1: a novel mechanism of Andersen syndrome. Cardiovasc Res 2007; 75:748-57.

10. Bendahhou S, Donaldson MR, Plaster NM, Tristani-Firouzi M, Fu YH, Ptacek LJ. Defective potassium channel Kir2.1 trafficking underlies Andersen-Tawil syndrome. J Biol Chem 2003; 278:51779-85.

11. Lopatin AN, Makhina EN, Nichols CG. The mechanism of inward rectification of potassium channels: "long-pore plugging" by cytoplasmic polyamines. J Gen Physiol 1995; 106:923-55.

12. Shieh RC. Mechanisms for the time-dependent decay of inward currents through cloned Kir2.1 channels expressed in Xenopus oocytes. J Physiol 2000; 526:241-52.

13. Nerbonne JM. Repolarizing cardiac potassium channels: multiple sites and mechanisms for CaMKII-mediated regulation. Heart Rhythm 2011; 8:938-41.

14. O'Hara T, Virag L, Varro A, Rudy Y. Simulation of the undiseased human cardiac ventricular action potential: model formulation and experimental validation. PLoS computational biology 2011; 7:1002061.

15. Kapa S, Tester DJ, Salisbury BA, Harris-Kerr C, Pungliya MS, Alders M, et al. Genetic testing for long-QT syndrome: distinguishing pathogenic mutations from benign variants. Circulation 2009; 120:1752-60.

16. Miake J, Marban E, Nuss HB. Functional role of inward rectifier current in heart probed by Kir2.1 over-expression and dominant-negative suppression. J Clin Invest 2003; 111:1529-36.

17. McLerie M, Lopatin AN. Dominant-negative suppression of I_{K1} in the mouse heart leads to altered cardiac excitability. J Mol Cell Cardiol 2003; 35:367-78.

18. Tristani-Firouzi M, Etheridge SP. Kir 2.1 channelopathies: the Andersen-Tawil syndrome. Pflugers Arch 2010; 460:289-94.

19. Lopes CM, Zhang H, Rohacs T, Jin T, Yang J, Logothetis DE. Alterations in conserved Kir channel-PIP_2 interactions underlie channelopathies. Neuron 2002; 34:933-44.

20. Ballester LY, Vanoye CG, George AL Jr. Exaggerated Mg^{2+} inhibition of Kir2.1 as a consequence of reduced PIP_2 sensitivity in Andersen syndrome. Channels (Austin) 2007; 1:209-17.

21. Ballester LY, Benson DW, Wong B, Law IH, Mathews KD, Vanoye CG, et al. Trafficking-competent and trafficking-defective KCNJ2 mutations in Andersen syndrome. Human mutation 2006; 27:388.

22. Foeger NC, Marionneau C, Nerbonne JM. Co-assembly of $K_v4\alpha$ subunits with K^+ channel-interacting protein 2 stabilizes protein expression and promotes surface retention of channel complexes. J Biol Chem 2010; 285:33413-22.

23. Yang KC, Foeger NC, Marionneau C, Jay PY, McMullen JR, Nerbonne JM. Homeostatic regulation of electrical excitability in physiological cardiac hypertrophy. J Physiol 2010; 588:5015-32.

24. Loussouarn G, Makhina EN, Rose T, Nichols CG. Structure and dynamics of the pore of inwardly rectifying K_{ATP} channels. J Biol Chem 2000; 275:1137-44.

25. Schrodinger LLC. The PyMOL Molecular Graphics System, Version 1.3r1. 2010.